

Comparison of surface treatment methods for promoting the adhesion of glass on titanium

P. VAN LANDUYT*, J.-M. STREYDIO, F. DELANNAY†

Université catholique de Louvain, Département des sciences des matériaux et des procédés, PCIM, place Sainte Barbe 2, 1348 Louvain-la-Neuve, Belgium
E-mail: vanlanduyt@ltp.dmx.epfl.ch

E. MUNTING

Unité de chirurgie orthopédique, Avenue Hippocrate 53, 1200 Bruxelles, Belgium

A glass allowing the wetting of titanium has previously been developed. Two surface treatments promoting glass adhesion on titanium are compared: preoxidation and phosphatation combined with preoxidation. After preoxidation at 700 °C, a 1 μm-thick TiO₂ layer covers titanium. The phosphated titanium substrates are oxidized at 600 °C to obtain a 20 μm-thick oxifluoride layer. After firing, glass adhesion is obtained with both surface treatments, but a "critical time of firing" appears with preoxidized titanium. WDS analysis suggests that diffusion of TiO₂ into the glass is responsible for adhesion on preoxidized titanium, while a complex oxifluoride layer allows redox phenomena in the case of phosphated titanium. Pull-off tests have measured a maximum strength from 1.5 to 3 MPa whatever the surface treatment. Measurement of transverse crack densities in the vitreous coatings gives a higher value for phosphated than for preoxidized titanium. This confirms that better adhesion is obtained after phosphatation treatment. © 1998 Kluwer Academic Publishers

1. Introduction

Bioceramics and bioglasses are well known for their bioactivity and ability to develop good bone bonding [1–3], but their brittleness constitutes a major limitation for load-bearing applications. Therefore they are used to cover metal (titanium, stainless steel or Co-Cr alloy) which constitutes the structural part of the implant. By coating the metal with a ceramics or vitreous layer, chemical leaching from the metal which can produce inflammatory response is avoided. Moreover, a non-bioactive surface is turned into a bioactive one which is able to bond with bone [4, 5]. Nowadays, bioactive coatings are more and more used in orthopaedics and dentistry.

In orthopaedics, fixation of the femoral part of the hip prosthesis remains a major problem for young patients. Whereas PMMA cements are largely used and give satisfactory results for old people with a duration of the prosthesis in the order of 10 to 15 years, this solution remains unsatisfactory in the case of young patients with a higher activity. New solutions involving plasma-sprayed hydroxyapatite (HAp) coatings on titanium have been developed during recent years in order to avoid the utilization of PMMA cements. Plasma-sprayed HAp coatings are bioactive and highly porous which makes possible bone ingrowth in the coating.

The major drawback of this kind of coating is the low mechanical properties: adhesion results in this case essentially from mechanical interlocking between the sand-blasted titanium surface and the ceramic layer. Thermal stresses resulting from the deposition process induce delamination of the coatings when the thickness increases [5].

Several attempts to realize new kinds of bioactive coatings on titanium are mentioned in the literature [5]. For example, Abe *et al.* have prepared apatite coatings deposited by a biological process on titanium [6]. Plasma spraying of bioglasses has been developed by Tranquilli Leali *et al.* [7]. Bioglasses reinforced with titanium particles are used by Ferraris *et al.* [8] to improve the strength of the plasma-sprayed coating. Several attempts to deposit coatings by enameling are also mentioned by Donald [9] in his general review on enameling processes. The high reactivity of titanium and the poor adhesion at the Ti/TiO₂ interface are major problems to be solved. Moreover titanium can reduce SiO₂ present in the glass to form brittle silicides. It is worth mentioning the work of Vast *et al.* [10] who have achieved good adhesion by enameling titanium with a P₂O₅-rich glass, as well as the contributions of Hautaniemi [11] and Pazo [12].

* *Current address:* Ecole Polytechnique Fédérale de Lausanne, Département des Matériaux, LTP, MX - Ecublens, 1015 Lausanne, Switzerland.

† Author to whom all correspondence should be addressed.

The aim of the present work is to develop a bioinert vitreous coating deposited on titanium. To achieve this, an enameling treatment is used which is hoped to present an improved adhesion compared to other methods [5–8]. This paper is focused on chemical adhesion and diffusion phenomena at the glass/titanium interface. Such bioinert vitreous coatings could be used as a chemical barrier to avoid leaching of metallic ions in the physiological environment. Moreover, fragments of HAp can be embedded in the glass to provide the bioactive properties of the implant surface. This composite coating (HAp/glass) should ensure a better bonding between the metal and HAp.

According to Pask [13], wetting of a metallic substrate by a glass enamel is improved by the addition of a metallic oxide of the substrate into the glass composition. Chemical adhesion is possible if chemical equilibrium is maintained through the interface thanks to diffusion or oxido-reduction reactions.

A glass composition which allows wetting of titanium has been selected during a previous work [14]. This paper focuses on the surface treatment of the metal and the firing treatment leading to adhesion of the vitreous coating. Two surface treatments are compared: a preoxidation of titanium at 700 °C giving a thin oxide layer (1 to 2 μm thickness) and a phosphatation treatment of the metal combined with a preoxidation at 600 °C producing a 10 to 20 μm -thick oxide layer. We will see that these two oxide layers are completely different regarding both their morphology and their composition. The firing treatment as well as the nature of the glass/titanium interface depend deeply on the previous surface treatment of the titanium substrate.

2. Materials and methods

2.1. Glass synthesis

The choice of the glass composition has been guided by the work of Pask [13] and is explained in detail elsewhere [14]. The aim was to prepare a glass presenting good wetting and adhesion properties on both titanium and HAp to be used as an intermediate layer. Because of the high reactivity of titanium, we have chosen a glass composition making possible a low enameling temperature, preferably below the α - β transition of titanium. For this reason, the basic components of the glass were SiO_2 - B_2O_3 - Na_2O . A borosilicate glass (SiO_2 - B_2O_3 - Na_2O - TiO_2) with a minimum content of 10 wt % TiO_2 has been used to favour wetting on titanium. The precise composition was adjusted to match the thermal expansion of the vitreous coating with that of titanium. In so doing, the residual stresses resulting from the enameling are minimized. Finally a glass with the following composition (wt %) was prepared: 46 SiO_2 -14 B_2O_3 -20 TiO_2 -11 Na_2O -5 F_2 . Fluorine was added to lower glass viscosity and reduce enameling temperature. The raw materials used were: SiO_2 , $\text{Na}_2\text{B}_4\text{O}_7$, Na_2CO_3 , Na_2SiF_6 and TiO_2 . Glass synthesis consists of two steps: raw materials decomposition for 3 h at 850 °C followed by fusion for 6 h at 1100 °C. Both operations were carried out in air in an alumina crucible placed in an electric furnace (Carbolite). The fused melt

TABLE I Surface treatments on titanium substrate

Surface cleaning	
Degreasing in acetone	
Decalamination in acid solution: 4 ml HF (38–40 vol%) 35 ml HNO_3 (70 vol%) 60 ml H_2O	
Samples I	Samples II
Preoxidation 1 h at 700 °C in air	Phosphatation in solution (100 ml) 4 g $\text{Na}_3\text{PO}_4 \cdot 12\text{H}_2\text{O}$ 1.1 g $\text{KF} \cdot 2\text{H}_2\text{O}$ 1.38 ml HF (38–40 vol%) Preoxidation 30 min at 600 °C in air

is then poured into water. The vitreous fragments are crushed in a planetary ball mill (PM4, Retsch) using agate jar and balls. 50 g-batch of glass powder so obtained is sieved and the fraction under 50 μm is used to process the coatings. Fluorescence X analysis reveals a 2–3 wt % contamination in Al_2O_3 which is not a major drawback as aluminium oxide is bioinert. The presence of Al_2O_3 increases glass viscosity slightly.

The toxicity of the glass was investigated by observing fibroblasts development on its surface. For this experiment, pellets of glass were pressed and sintered at 700 °C for 5 minutes. The sintered pellets were left during 1 week in contact with the cell culture. They were completely covered by fibroblasts at the end of the week. The cells were superimposed in several layers which proved their affinity for the glass.

2.2. Surface treatment of titanium

Use is made of 1 mm-thick commercially pure titanium sheets (grade 2–ASTM B-265–minimum Ti content of 98.9 wt %, Philip Cornes & Co. Ltd., Belgium). The successive stages of surface treatment of the titanium substrates are performed in several solutions whose composition is given in detail in Table I. The titanium surface is first degreased with acetone. The samples are subsequently dipped during 5 min in a diluted acid solution based on a mixture of HF and HNO_3 in order to dissolve the oxide layer resulting from the rolling of the metal. Then, two different surface treatments are carried out in air in an electric furnace. The so-called samples I are preoxidized for 1 h at 700 °C. Samples II are dipped for 20 min in a phosphatation solution heated at 85 °C. Thereafter, these samples are preoxidized for 30 min at 600 °C.

The thickness of preoxidation layers was calculated from Archimedean measurements which avoided the need of an hypothesis about their density.

2.3. Coating and firing processes

A thin uniform layer of glass powder is first obtained by sedimentation of glass powder onto the pre-treated titanium substrates. For this purpose, a suspension is obtained by dispersing sieved glass powder in methylethylketone (MEK) using a magnetic stirrer. Then, the titanium substrates are placed on the bottom of the suspension and sedimentation is allowed for

about 12 h. The coated samples are dried in air or in an oven at 120 °C during 3–4 h to eliminate residual MEK. The quantity of glass powder dispersed in MEK is adjusted in order to obtain a 60 μm -thick vitreous coating after firing.

Firing is carried out in an electric furnace at 700 °C in air for different durations depending on the previous surface treatments of titanium. In the case of samples I, enameling conditions have been investigated for temperatures ranging from 650 to 850 °C by steps of 50 °C during increasing times. The phosphated samples II were fired at 700 or 730 °C for different durations.

2.4. Characterization of the interface

Glass/titanium interfaces were studied by scanning electron microscopy (SEM) and the oxide composition along profiles perpendicular to the interface was analysed using Wave Dispersing Spectrometry (WDS). The nature of the oxide layer resulting from preoxidation was determined by X-ray diffraction combined with WDS.

2.5. Mechanical testing

Adhesion of the vitreous coatings was characterized by means of two mechanical tests which give complementary information. Our aim was to compare the efficiency of the two surface treatments. The specimens used for mechanical testing were prepared according to the following conditions: samples I and II were fired at 700 °C during 5 and 30 min, respectively. The thickness of the vitreous coatings was about 60 μm , while titanium substrate thickness was 1 mm. First, pull-off tests (ASTM C633) were carried out in order to compare the adhesion of our samples with that of plasma-sprayed HAP coatings. For these tests, 25 mm diameter disc samples were covered with glass. Studs of 22 mm-diameter Inconel 600 were glued with Araldite adhesive on each face of the samples. Polymerization of Araldite adhesive was allowed for 3–4 hours at 40 °C in an oven. The studs were clamped in the grips of the testing machine. Careful alignment of the two studs is of uttermost importance for the reliability of the pull-off test. Perfect alignment is indeed necessary to ensure the absence of bending or shearing along the interface, in such a way to warrant decohesion in mode I. The tension load was applied using a Zwick testing machine with a strain rate of 1 mm/min. The maximum load in traction was registered and the fracture profiles after decohesion were observed with a stereomicroscope.

Secondly, transverse crack extension through the thickness of the layer was studied in tension (Fig. 1). Coated sheets of 150 mm length, 15 mm width were loaded in tension with a strain rate of 0.1 mm/min. An extensometer followed the straining of the sheets. For every 1% of deformation, straining was stopped and the number of transverse cracks was counted with the help of a zoom camera. This test also allows the distinction between transverse and interfacial debond cracks.

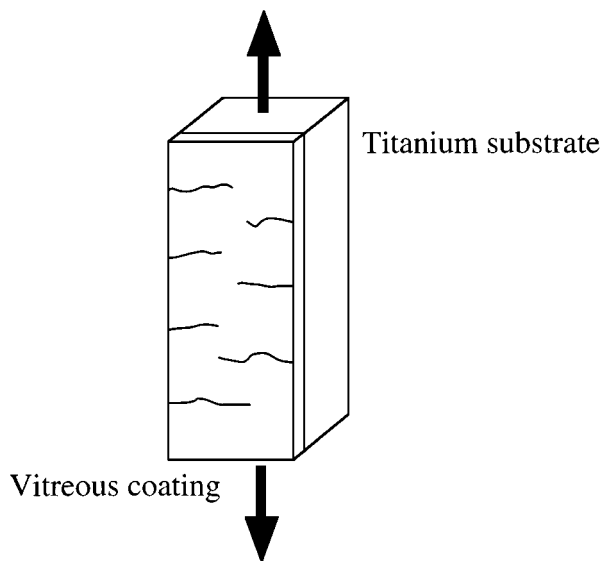


Figure 1 Measurement of transverse crack evolution in tension.

3. Results

3.1. Preoxidation

3.1.1. Titanium surface treatment

X-ray diffraction analysis indicated that the dark-gray colored layer obtained after preoxidation treatment during 1 h at 700 °C was made of TiO_2 -rutile. The thickness of the layer was about 1 to 2 μm .

3.1.2. Enameling conditions

A systematic study of firing conditions was carried out. Different times of firing at temperatures varying from 650 °C to 850 °C by steps of 50 °C were investigated. For each temperature, we determined the critical time of firing beyond which spontaneous decohesion of the coating occurs during cooling of the sample to room temperature. When such a spontaneous decohesion has occurred, the titanium substrate appears to have completely been deoxidized under the vitreous coating. Fig. 2 shows the variation of this “critical time of firing” as a function of the enameling temperature for titanium sheets covered with a 1 to 2 μm -thick TiO_2 layer. The curve delineates two domains: spontaneous decohesion is observed only above the curve. The same experiment

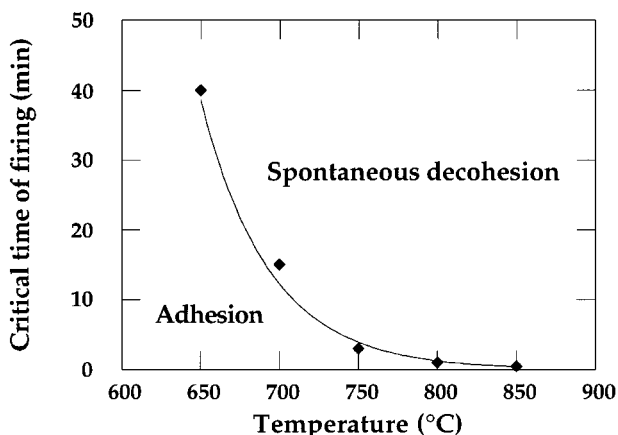


Figure 2 Critical time of firing versus enameling temperature for pre-oxidized samples.

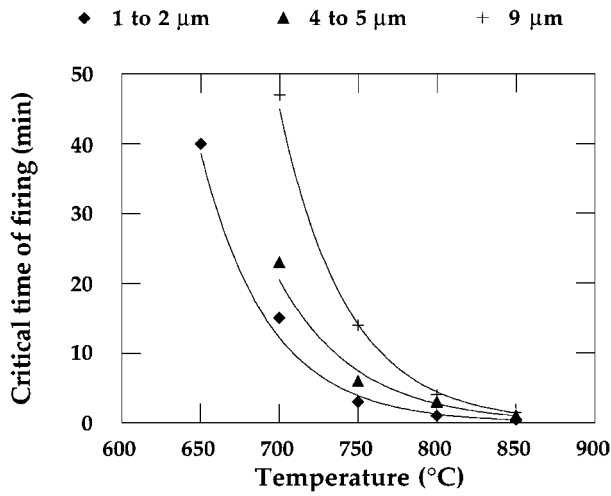


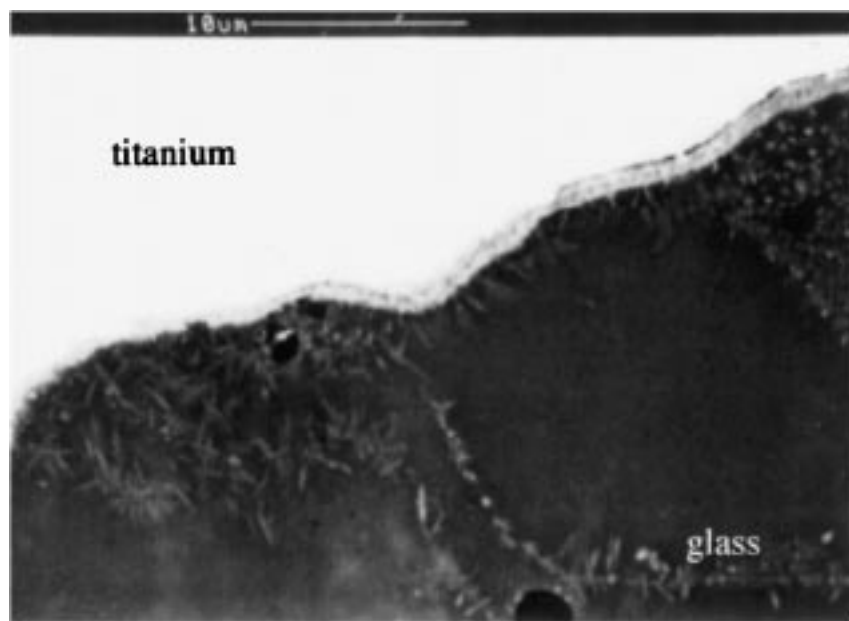
Figure 3 Critical time of firing versus enameling temperature for different TiO_2 layer thicknesses (preoxidized samples).

was made for increasing thicknesses of the TiO_2 pre-oxidation layer. Thicknesses of 1–2 μm and 4–5 μm are obtained after preoxidation at 700 °C during 1 and 4 h respectively, while a thickness of 9 μm is obtained after a preoxidation at 800 °C during 1 h. As shown in Fig. 3, the same kind of curve is obtained for different TiO_2 -layer thicknesses. The critical time for spontaneous decohesion during cooling to room temperature increases with increasing thickness of the oxide layer.

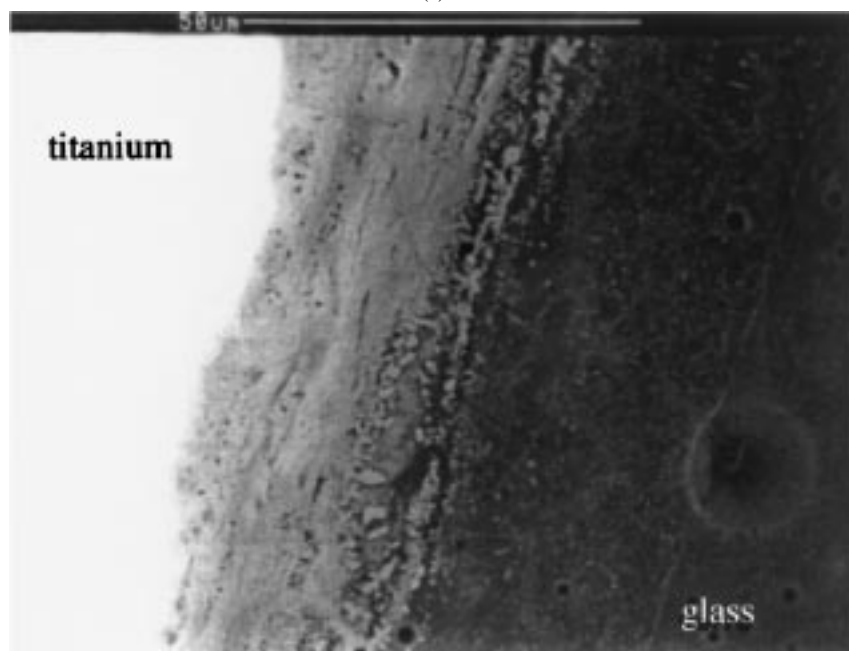
3.1.3. Characterization of the interface

Fig. 4a shows the microstructure of the interfaces of pre-oxidized samples. Preoxidized samples enameled during 5 min at 700 °C present a thin continuous TiO_2 -layer between glass and titanium.

As shown in Fig. 5a, the WDS profile of the interface gives evidence of some diffusion of TiO_2 in the glass.



(a)



(b)

Figure 4 Microstructure of the interface for (a) preoxidized samples and (b) phosphated samples.

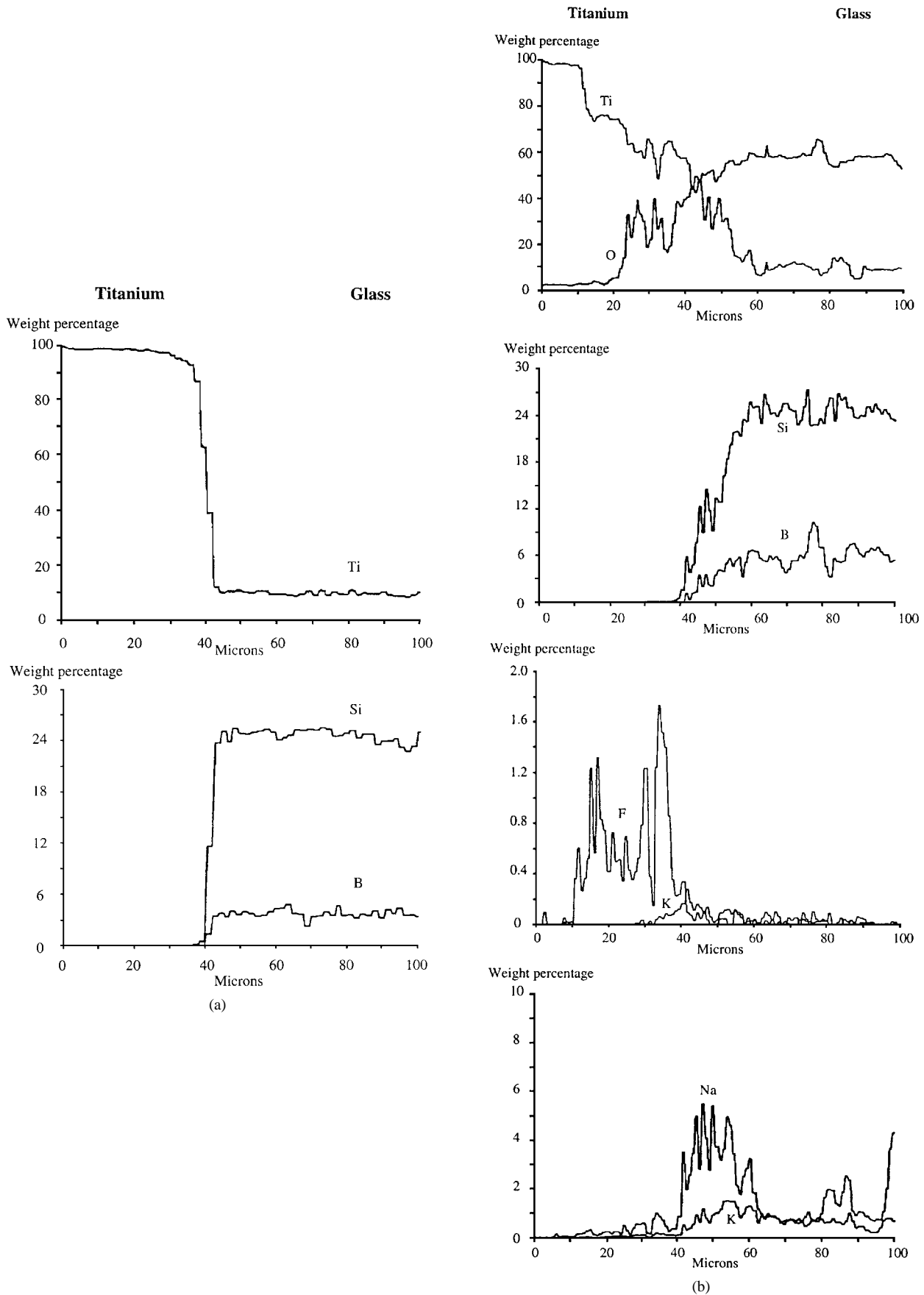


Figure 5 WDS analysis of the interface of (a) preoxidized samples and (b) phosphated samples.

3.2. Phosphatation

3.2.1. Titanium surface treatment

For the samples pretreated by phosphatation, WDS indicated the presence of a sub-micrometer layer con-

taining Na, K, P and F on titanium surface. The main property of this gray layer appeared to be the acceleration of the oxidation kinetics of titanium. Preoxidation during 30 min at 600 °C was sufficient to bring about

the growth of a 15 to 20 μm thick white-yellow layer. This layer is a complex mixture of TiO_2 (rutile) and fluorine. We will call this layer "oxifluoride". K, Na and P were found to remain on the surface of this oxifluoride layer. This means that, during oxidation, the oxifluoride layer grows between the phosphatation layer and the Ti substrate while F incorporates into TiO_2 .

3.2.2. Enameling conditions

The behaviour of phosphated samples after firing is different from that of preoxidized samples. Whatever the time of firing at 700°C , no spontaneous decohesion is observed. Samples enamelled during 1 h 30 at 730°C did also not exhibit spontaneous decohesion.

3.2.3. Characterization of the interface

Fig. 4b shows that the oxifluoride layer formed on phosphated sheets is thicker than on preoxidized sheets,

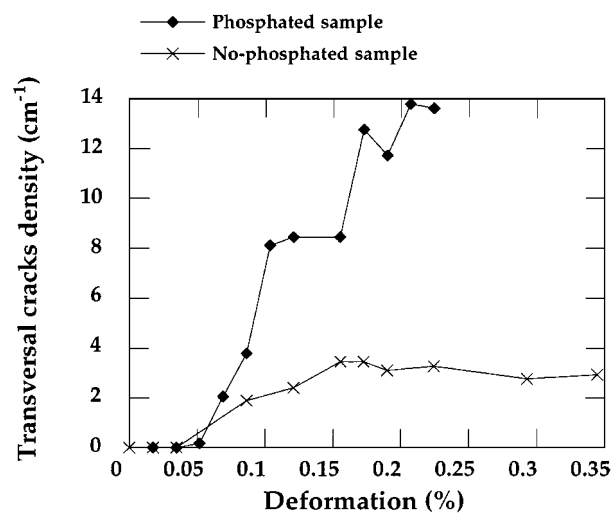


Figure 6 Comparison of transverse crack densities for preoxidized and phosphated samples.

is quite regular and presents a lamellar structure with some porosity.

As shown in Fig. 5b, WDS profiles of phosphated samples are quite intricate. Several elements such as K, Na, F and P originate from the phosphatation treatment while others such as Si, B, Na, Ti and O come from the glass. The WDS profiles show how these elements mix during enameling. From the left to the right hand side, the titanium substrate, the Ti-F-O oxifluoride layer, a P, K and Na-rich layer and finally a layer consisting of a continuous diffusion of K and Ti into the glass can be observed. It can be noticed that P is quite localized between the oxifluoride layer and the glass itself.

3.3. Mechanical tests

Pull-off tests measured a maximum strength in the range from 1.5 to 3 MPa (± 1 MPa). This value is quite low and exhibits a large dispersion. The observation of the fracture surface shows that delamination takes place between the titanium substrate and the TiO_2 -layer for the preoxidized samples.

During the pull-off tests on the phosphated sheets, debond crack propagates in the middle of the oxifluoride layer. Moreover, decohesion is limited at the glued surface in the case of phosphated samples while it extends to the whole surface for preoxidized samples.

Fig. 6 compares transverse crack densities for preoxidized and phosphated samples. Under increasing straining of the sheet in tension, transverse cracks on the preoxidized samples begin to appear for a critical strain ϵ_c (around 0.05%) whatever the samples preparation method. As illustrated in Fig. 7, a pattern of parallel cracks forms progressively. The number of transverse cracks stabilizes for a strain of 0.15% in the case of preoxidized samples. The final density of transverse cracks reaches 3 cm^{-1} .

On phosphated samples, transverse crack density stabilizes at a value of 14 cm^{-1} for a strain of 0.20%. This means that, for phosphated samples, the minimum

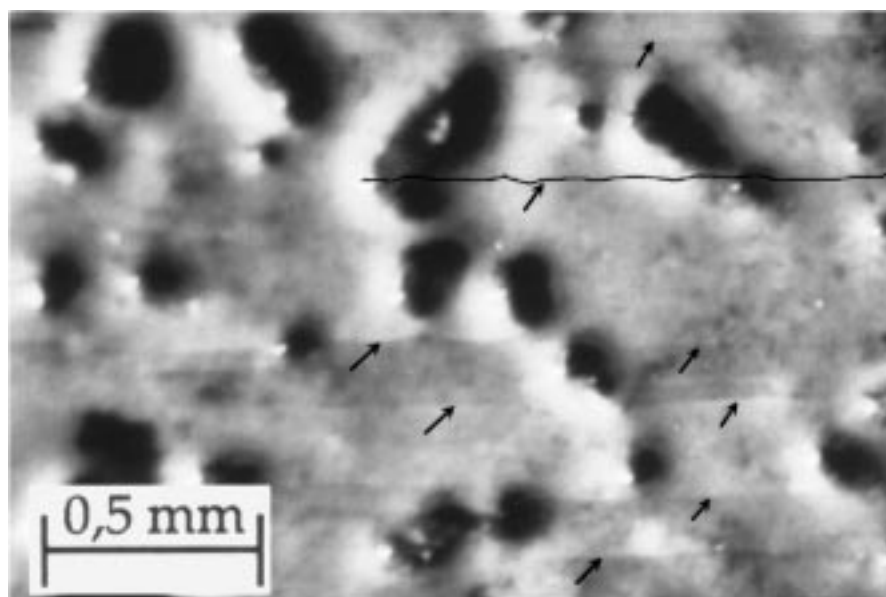


Figure 7 Pattern of parallel cracks on phosphated sample.

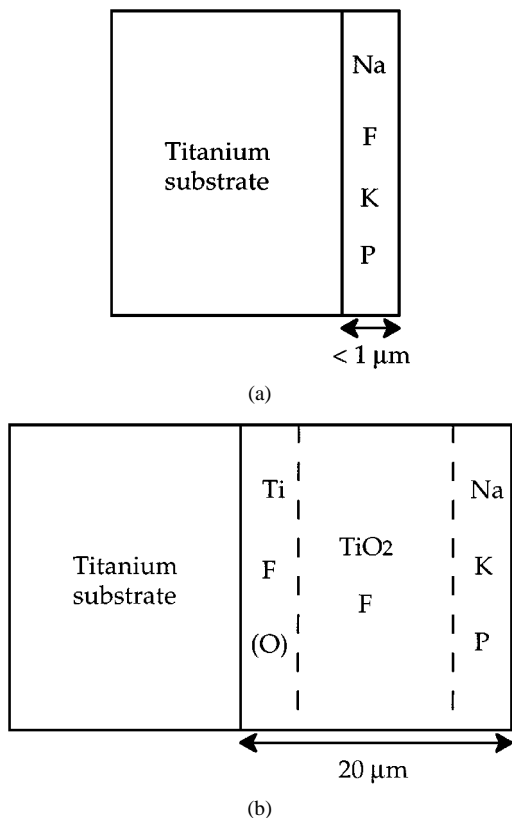


Figure 8 Distribution of K, P, Na, F, Ti and O (a) after phosphatation, (b) after phosphatation and oxidation.

average crack interdistance is about equal to the thickness of the coating ($60 \mu\text{m}$).

4. Discussion

4.1. Titanium surface treatments

Preoxidation induces the formation of a TiO_2 -rutile layer on samples I. X-ray diffraction indicates that the combination of phosphatation and preoxidation treatment carried out for samples II produces a mixture of TiO_2 -rutile with another non-identified crystalline phase. WDS analysis shows, that after oxidation at 600°C , fluorine has disappeared from the oxifluoride layer. As sketched in Fig. 8, we propose that the oxifluoride layer grows under the phosphatation layer. The most remarkable effects of the phosphatation treatment are thus an increase of the kinetics of oxidation and a modification of the nature of the oxidation layer.

4.2. Contributions to adhesion

4.2.1. Critical time of enameling

The complete deoxidation of titanium before a spontaneous decohesion of the coating occurs and the increase of the critical time of firing with the thickness of initial oxide layer suggests that adhesion is promoted by diffusion of the TiO_2 -layer into the glass. The layer does not regenerate during enameling and no oxido-reduction reactions are evidenced. Hence spontaneous decohesion occurs after complete exhaustion of the TiO_2 layer. The variation of the critical time for decohesion versus temperature (Fig. 2) can be translated into the Arrhenius diagram shown in Fig. 9. The slope of the straight lines corresponds to the activation energy for diffusion

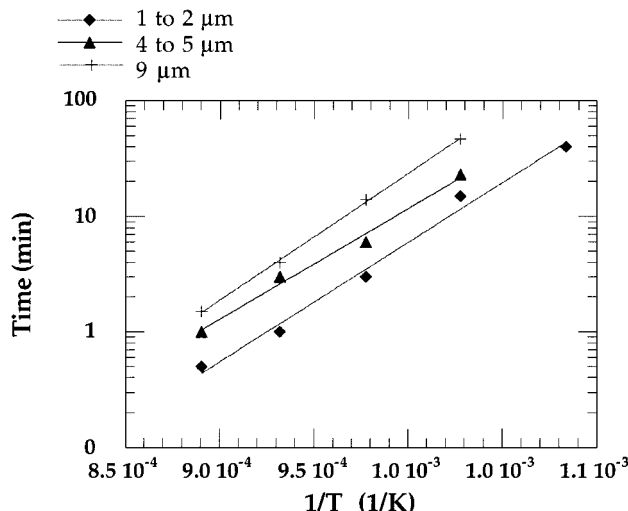


Figure 9 Arrhenius diagram.

of TiO_2 in the glass. The parallelism of the lines, whatever the thickness of the oxide layer shows that the activation energy is independent of the oxide thickness. Diffusion profiles of TiO_2 into glass have been fitted by error functions in such a way that they determine the diffusion coefficient D of TiO_2 in the glass. The calculated value of $D = 3.5 \pm 0.5 \cdot 10^{-11} \text{ cm}^2/\text{s}$ (750°C) [14] agrees with the value of D obtained by Eppler [15]. Adhesion should solely result from a diffusion phenomena in the case of samples I.

4.2.2. Phosphatation treatment

Diffusion is not the only promoter of adhesion in the case of samples II. The initial "oxifluoride" layer being thicker than the rutile layer of samples I, extrapolation of the curves of Fig. 3 suggests a critical time of about 50 min for this layer thickness. Experimentally, no spontaneous decohesion appears even after enameling during 90 min at 730°C . Moreover, WDS profiles (Fig. 5b) do not suggest extensive diffusion of Ti into the glass. We have schematically drawn in Fig. 10 the distribution of the elements as given by WDS analyses. One can notice that P, although present in minor quantity, segregates between F and Si, B, i.e. between the oxifluoride layer and the glass. We may thus speculate that oxido-reduction reactions between Ti and P occur and contribute to the equilibrium favoring adhesion. Indeed, reduction of Ti^{4+} in Ti^{3+} by P has been evidenced by P. Vast in another glass [10].

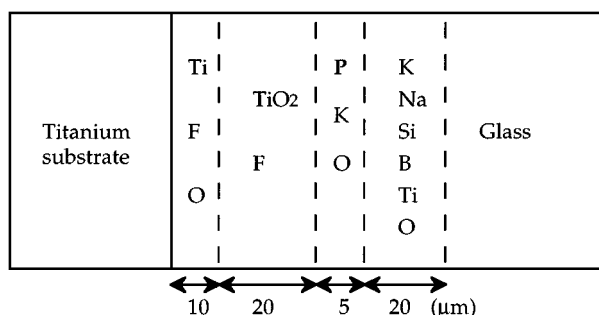


Figure 10 Outline of the phosphated sample interface.

4.3. Toxicity test

Fibroblast culture only consists of a preliminary test for assessing toxicity. This test alone does not allow to claim that the glass composition used in this work is truly biocompatible. It is however an encouraging result. None of the oxides components is known to be toxic. The behaviour of this glass when placed in the human body, will depend very much on the quantity of ions released. The chemical stability of the glass is thus a determining factor. If this glass is indeed sufficiently bioinert, the biocompatibility of the coating could be further promoted by embedding of hydroxyapatite fragments in it.

4.4. Adhesion strength

The real significance of pull-off tests may be questionable because of the difficulty of guaranteeing mode I fracture. Nevertheless adhesion strengths were far lower than those measured on plasma-sprayed HAP which varies usually from 10 to 30 MPa [16–19]. According to Ashcroft, the maximal strength of a vitro-ceramic enamel can reach 35–52 MPa meanwhile plasma-sprayed HAP value is 11 MPa according to Pollier and varies from 33 to 52 MPa according Chern Lin. Numerous factors are against a high relevance of values obtained by this test. Critical factors are for instance the quantity of adhesive, the size of the stud, the residual stresses in the coating, the perfect alignment of the system.

In contrast, the measurement of transverse crack evolution in tension allows comparison of the interfacial resistance to crack propagation [20, 21]. Actually, transverse cracks appear in the coating at a critical deformation ε_c . ε_c increases when the modulus and thickness of the coating decrease in comparison to those of the substrate. When the crack density increases, the energy release rate decreases progressively in such a way that the successive cracks will statistically appear at equal distance from two existing cracks having propagated earlier. Cracks propagate thus in successive patterns. When a transverse crack reaches the interface, its behaviour depends on the toughness of this interface. When interface toughness is low, the crack deviates and propagates along the interface. Interfacial propagation allows an increase of the energy release rate and reduces the possibilities of cracking in the vicinity of a previous crack. The maximum transverse crack density thus reflects the ease of interfacial decohesion. The easier the interfacial decohesion, the lower the crack density. In the absence of decohesion, the minimum distance between cracks is of the order of the layer thickness. This is observed in the case of phosphated samples. It is thus obvious that phosphated samples resist better to interfacial crack propagation, which attests the fact that adhesion is improved. Nevertheless, the final cracks density remains lower than that obtained by Boland *et al.* [21] on plasma-sprayed coatings.

5. Conclusions

Enameling of titanium sets quite intricate problems. By analyzing both interfaces, we have highlighted the

different mechanisms responsible of adhesion achievement. In the case of preoxidation at 700 °C, solely diffusion of TiO₂-layer into the glass is responsible for adhesion, while phosphatation treatment should allow achievement of chemical equilibrium along the interface.

Mechanical testings have revealed behaviour directly related to the surface treatment of titanium and tend to prove that phosphatation treatment improves adhesion. Fair adhesion can easily be obtained by a preoxidation treatment of the substrate but the first limitation is the intrinsically poor adhesion between TiO₂ and titanium. This work demonstrates that the mere diffusion of TiO₂ in the coating can not lead to sufficient adhesion. Phosphatation treatments gives a much thicker oxifluoride interfacial layer. Cracks propagation measurements in the oxifluoride layer clearly show a better adhesion. Minimization of the thickness of this oxifluoride layer could lead to improvement of adhesion.

Minor additions of P₂O₅ in the glass should be attempted in order to favour oxido-reduction reactions. Although chemical adhesion between glass and titanium measured in the present work remains lower than mechanical adhesion between HAP plasma-sprayed coatings, it should be kept in mind that combinations of both chemical and mechanical adhesion by enameling sand blasted titanium substrates should improve very much the situation and allow valid comparison between the two types of coatings.

Acknowledgements

This work has been carried out with financial support of FDS-UCL and of SSTC (Belgium) in the framework of PAI 41. N. Heylen is thanked for the toxicity tests. The Centre des Matériaux P.M. Fourt (Ecole des Mines de Paris) is thanked for WDS measurements.

References

1. L. L. HENCH and J. WILSON, *MRS Bulletin*, Sept. 1991, pp. 62–74.
2. R. H. DOREMUS, *J. Mater. Sc.* **27** (1992) 285–297.
3. W. SUCHANEK and M. YOSHIMURA, *J. Mater. Res.* **13** (1) (1998) 94–113.
4. R. M. PILLIAR, J. E. DAVIES and D. C. SMITH, *MRS Bulletin*, Sept. 1991, pp. 55–61.
5. A. RAVAGLIOLI and A. KRAJEWSKI, "Bioceramics—Materials, Properties, Applications" (Chapman & Hall, 1992) pp. 198–244.
6. Y. ABE, T. KOKUBO and T. YAMAMURO, *J. Mater. Sc.: Mater. in Med.* **1** (1990) 233–238.
7. P. TRANQUILLI LEALI, A. MORELLI, O. PALMACCI, C. GABBI, A. CACCHIOLI and G. GONIZZI, *ibid.* **5** (1994) 345–349.
8. M. FERRARIS, C. BADINI and B. COUZINET, *Composites* **25** (7) (1994) 494–498.
9. I. W. DONALD, *J. Mater. Sc.* **28** (1993) 2841–2886.
10. P. VAST, *J. de Physique IV*, colloque C7, supplément au *J. de Phys.* **III 3** (1993).
11. J. A. HAUTANIEMI, H. HERO and J. T. JUHANOJA, *J. Mater. Sc.: Mater. in Med.* **3** (1992) 186–191.
12. A. PAZO, E. SAIZ and A. P. TOMSIA, *Acta Mater.* **46** (7) (1998) 2551–2558.
13. J. A. PASK, *Ceramic Bulletin* **66** (11) (1987) 1587–1592.
14. P. VAN LANDUYT, J.-M. STREYDIO, F. DELANNAY and E. MUNTING, *Clinical Materials* **17** (1994) 29–33.

15. R. A. EPPLER and G. H. SPENCER-STRONG, *J. Amer. Ceram. Soc.* **52** (1969) 263–266.
16. I. A. ASHCROFT and B. DERBY, *J. Mater. Sc.* **28** (1993) 2989–2998.
17. M. J. FILLIAGGI and R. M. PILLIAR, *J. Mater. Sc.* **26** (1991) 5383–5395.
18. J. H. CHERN LIN, M. L. LIU and C. P. JU, *J. Mater. Sc.: Mater. in Med.* **5** (1994) 279–283.
19. N. POLLIER, private communication.
20. F. DELANNAY and P. WARREN, *Acta Metall. Mater.* **39** (1991) 1061–1072.
21. F. BOLAND, F. LI, G. SCHNEDECKER, M. BONCOEUR and F. DELANNAY, *Silicates Industriels* **57** (1992) 108–112.

Received 12 September 1997

and accepted 1 June 1998